Inertia in Renewable Power Systems: A Review of Estimation Methods and Prac-tical Implementation

Mehrzad, Alireza ; Darmiani, Milad ; Rouhani, Seyed Hossein ; Su, Chun-Lien; Sepestanaki, Mohammadreza Askari; Mofidipour, Erfan ; Monti, Antonello; Anvari-Moghaddam, Amjad

Published in:
Renewable & Sustainable Energy Reviews

DOI (link to publication from Publisher):
10.1016/j.rser.2025.116246

Publication date:
2026

Document Version
Publisher's PDF, also known as Version of record

Renewable and Sustainable Energy Reviews 226 (2026) 116246

Contents lists available at ScienceDirect

Renewable and Sustainable Energy Reviews

journal homepage: www.elsevier.com/locate/rser

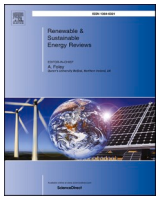

Inertia in renewable power systems: a review of estimation methods and practical implementation

Alireza Mehrzad [a], Milad Darmiani [a], Seyed Hossein Rouhani [a], Chun-Lien Su [a,*], Mohammadreza Askari Sepestanaki [a], Erfan Mofidipour [b], Antonello Monti [c], Amjad Anvari-Moghaddam [d]

[a] Department of Electrical Engineering, National Kaohsiung University of Science and Technology, Kaohsiung, Taiwan
[b] Department of Energy, Amirkabir University of Technology, Tehran, Iran
[c] Institute for Automation of Complex Power Systems, RWTH Aachen University, Aachen, Germany
[d] Department of Energy (AAU Energy), Aalborg University, Aalborg, Denmark

ARTICLE INFO

Keywords:
Inertia estimation
Measurement-based inertia estimation
Model-based inertia estimation
Artificial intelligent-based inertia estimation
Low-inertia power system
Frequency response
Renewable energy sources

ABSTRACT

The dynamic behavior of modern power systems is being fundamentally reshaped by the increasing penetration of renewable energy sources with low or zero inertia, such as wind and solar PV. Consequently, in many regions, the rotational inertia traditionally provided by conventional synchronous generators has significantly declined. Since virtual inertia–achieved through synthetic inertia control– is not yet widely implemented, the overall system inertia has fallen well below that of traditional power systems. Accurate estimation of critically low inertia levels is therefore essential to ensure reliable and stable system operation. This review paper presents a comprehensive assessment of existing methods for inertia estimation in both conventional and renewable-rich power systems. It systematically compares techniques adopted by utilities, highlighting their practical applications, strengths, and limitations. Furthermore, the paper evaluates the feasibility of these approaches from an implementation perspective and discusses emerging challenges. Finally, it outlines future directions toward robust, adaptive, and real-time inertia estimation methods capable of supporting the secure operation of next-generation power systems.

1. Introduction

Energy systems globally are shifting towards Renewable Energy Sources (RESs) to achieve net-zero emissions by 2050 [1]. Concerns have emerged regarding the reliability and sustainability of power systems as traditional generators, which rely on the rotational inertia of large machines, are being replaced by low-inertia RES connected through power converters [2]. This transition leads to reduced system inertia, an increased Rate of Change of Frequency (RoCoF), a lower frequency nadir, the risk of Under Frequency Load Shedding (UFLS), the tripping of generator protection devices, and heightened system security threats [3–6]. Low-inertia RES connects to the grid through converters that can be operated in grid-forming mode to provide Virtual Inertia (VI) by adapting their output active power in accordance with the RoCoF, thereby emulating the Synchronous Generator (SG) inertia response based on frequency deviations [7,8]. Adding VI to a modern power system can compensate for the lack of a fast response from Primary Frequency Control (PFC) to system frequency changes within a timeframe of less than 10 s. Transmission Systems Operators (TSOs) need real-time information on the level of inertia for control, planning, and stable operation of the grid. Therefore, precise inertia estimation is important and essential for integrating renewables, ensuring grid stability, optimizing generation dispatch, and improving economic efficiency [2,9].

The issue of inertia estimation was first addressed by Inoue et al., in 1997 [10], who proposed a fifth-order polynomial approximation for estimating RoCoF over 15–20 s following generator and load losses. Initial estimates often exceeded the actual generator inertia constants. While a swing equation was later developed to link load with estimated inertia, accuracy suffered due to the lack of substantial disturbances [11]. Efforts to improve estimation included analyzing multiple locations and substituting known disturbances with power data, but success

* Corresponding author.
E-mail address: cls@nkust.edu.tw (C.-L. Su).

https://doi.org/10.1016/j.rser.2025.116246
Received 1 May 2025; Received in revised form 19 August 2025; Accepted 24 August 2025

still depended on the precise identification of disturbance onset and optimal sliding window sizes [12]. Although setting a 20 ms window improved accuracy, it does not account for Converter-Interfaced Generations (CIGs), highlighting the need for insights into the size and temporal distribution of power imbalances [13]. An online inertia estimation method using PMUs and integrating SGs and photovoltaic sources via Virtual Synchronous Generators (VSG) was proposed but remained influenced by modes, window length, and Fourier coefficients [14]. Some systems, like the Nordic system, estimate kinetic energy through SCADA by tracking circuit breaker positions and generator power, but they neglect virtual inertia and load contributions [3,15]. Real-time tools are employed in ERCOT, Ireland, and the UK, while Japan assesses inertia via transient events due to RES [16]. Inertia estimation methods are reviewed based on time horizons and scopes, focusing on synchronous generators or measurement techniques [17–20]. However, practical implementation challenges remain largely unaddressed, and innovative approaches, such as artificial intelligence, have not been sufficiently explored for inertia estimation in renewable systems.

This paper reviews the latest techniques for estimating inertia in renewable power systems, presenting and discussing state-of-the-art strategies. To enhance estimation robustness against detailed system models and uncertainties, such as network line parameters, most approaches rely on measurement- and forecasting-based methods. This paper bridges the gap between model-based, measurement-based, and forecasting-based estimation techniques and their practical implementation by research institutes and TSOs. It also provides insights into load side inertia estimation and highlights future trends toward robust, adaptive, and real-time techniques for renewable power systems. This study contributes to the literature as follows:

- Provides a comprehensive evaluation of the merits and limitations of existing studies on inertia estimation, covering model-based, measurement-based, and artificial intelligence–based approaches. This offers valuable insights for researchers regarding the implementation and application of different inertia estimation methods.
- Presents a detailed discussion and assessment of measurement-based methods, examining inertia contributions from SGs, CIGs, and the demand side.
- Compares existing studies from multiple perspectives, including estimation accuracy, the sources of inertia considered, and the operating conditions under which the methods are applied.
- Explores the integration of demand-side virtual inertia, with particular attention to the future expansion of electric vehicle-to-grid (V2G) schemes.
- Investigates current practical inertia estimation methods adopted by power companies, highlighting real-world implementation challenges and practices.

The remaining sections of this paper are arranged as follows. Section 2 of this paper outlines definitions of power system inertia in both traditional and modern power systems. Next, an examination of how inertia operates in these systems and the difficulties it faces when RESs are added will be conducted. Section 3 evaluates various estimation methods, classifies them, and discusses their respective advantages and limitations. Section 4 presents the current practical strategies reviewed in this study, while Section 5 summarizes the key findings from the literature. Section 6 is devoted to the challenges associated with real-time inertia estimation tools. Section 7 addresses the main challenges and future perspectives for inertia in RES-dominated power systems. Finally, Section 8 offers concluding remarks and outlines directions for future research.

2. Inertia in renewable power systems

Inertia is one of the fundamental properties of a power system as it limits the RoCoF and frequency nadir. The SG rotational masses provide inertia in traditional power systems [2,21]. Rotational inertia prevents rapid fluctuations in system frequency caused by imbalances between power generation and consumption, manifested through any form of energy exchange [22]. The kinetic energy contained in a rotating mass of generators is traditionally released after a power imbalance. Inertia is characterized by the kinetic energy E_{kin}, which is stored in the rotating mass at the specified speed and is then divided by the rated power of machine S_B, as indicated in:

$$H = \frac{E_{kin}}{S_B} = \frac{J(2\pi f_m)^2}{2\,S_B} \tag{1}$$

where H is the inertia constant of the machine in seconds, J represents the moment of inertia of the shaft in $kg.\,m^2$ and f_m is the machine-rated rotational frequency. ω_n indicates the nominal speed in rad/s equivalent to $2\pi f_m$ [21,23]. The range of usual inertia constants in a power system is 1.75 s to about 10 s, with variations depending on the type of conventional unit being considered (e.g., steam, combined cycle, hydroelectric, etc.). Lately, operators of various low-inertia systems around the world have implemented rapid frequency response services that demand a response to a frequency deviation in 1–2 s [17].

The transient response of the system frequency following a power imbalance event is typically modeled using the generator swing equation. For the traditional power system, the swing equation can be represented as:

$$2H_{eq}\frac{d\Delta f}{dt} = \Delta P_m - \Delta P_e = \Delta P_m - \Delta P_L - D\Delta f \tag{2}$$

where Δf is the grid frequency deviation, ΔP_m stands for the total mechanical power change provided by the generators, and ΔP_e is the overall electrical power deviation of the entire power system [18].

Certain electrical loads, such as rotating machinery, are frequency-dependent. As a result, the expression for ΔP_e is $\Delta P_e = \Delta P_L + D\Delta f$, where ΔP_L represents the power variation of loads that are not dependent on frequency and D is the damping factor (load-frequency response constant). RoCoF is denoted as $\frac{d\Delta f}{dt}$. On the other hand, in renewable power systems integrating RESs, the inertia response, E_t^I, is made up of two primary components, including the kinetic energy in rotating masses synchronized with the power system, $E_t^{I,SG}$, and the VI provided by converter-interfaced generation, $E_t^{I,CIG}$ [17]:

$$E_t^I = E_t^{I,SG} + E_t^{I,CIG} \tag{3}$$

For grid-forming converter interfaced generation, the VSG control is responsible for inertia response by emulating the SGs dynamic behavior based on swing equation, as:

$$\frac{2H_{VSG}S_{VSG}}{\omega_0}\,\dot{\omega}_{VSG}(t) = P_{set} - P_e(t) - \frac{1}{1+sT_c}K_{VSG}\Delta\omega(t) \tag{4}$$

where H_{VSG} represents the emulated inertia in seconds, S_{VSG} denotes the rated power of VSG, ω_{VSG} indicates the converter internal speed reference in per-unit, P_{set} specifies the active power generation set-point in per-unit, P_e is the converter active power output in per-unit, T_c is the time constant, and K_{VSG} quantifies the emulated damping coefficient [3,7].

In DC systems, the concept of inertia operates differently compared to AC systems. As mentioned, in AC systems, inertia relates to the rotating masses of generators and motors, resisting frequency changes. However, in DC systems, which lack rotating machinery, inertia relates to RESs and Energy Storage Systems (ESSs), such as batteries or capacitors, that regulate voltage and respond to rapid changes in load or generation [24]. Power balance formulation in DC systems is expressed as follows:

$$C \cdot u_{dc} \cdot \frac{du_{dc}}{dt} = P_{in} - P_{out} - P_c \tag{5}$$

where C indicates the dc bus capacitor, u_{dc} is the dc bus voltage, P_{in} is the converter output power, P_{out} represents the power flows to the dc bus, and P_c demonstrates the capacitor power charging. The capacitor is responsible for storing energy, which provides active power to reduce the Rate of Change of Voltage (RoCoV) and to improve voltage stability. The stored energy and the inertia time constant are formulated as follows:

$$H_{dc} = \frac{E_{cap}}{S_{Nc}} = \frac{1}{2}\frac{C{u_{dc}}^2}{S_{Nc}} \tag{6}$$

where S_{Nc} is the rated capacity of capacitors.

In hybrid renewable power systems incorporating both DC and AC components, the DC-side inertia interacts with the AC system through power converters, which emulate the behavior of synchronous generators. Due to the mixture of SGs, ESSs, and RESs, the total inertia of the hybrid power system includes both the synchronous inertia from the SG and the virtual inertia from the RES and ESS. Hence, the equivalent inertia H_{eq} can be represented as shown in the following equation [19]:

$$H_{eq} = \frac{\sum_{i=1}^{N_{SG}} H_{SG,i}S_{B,i} + \sum_{j=1}^{N_{CIG}} H_{CIG,j}S_{B,j}}{\sum_{i=1}^{N_{SG}} S_{B,i} + \sum_{j=1}^{N_{CIG}} S_{B,j}} \tag{7}$$

where $H_{SG,i}$, $S_{B,i}$, $S_{B,j}$, and $H_{CIG,j}$ stand for the inertia constant of power plant, rated power of plant i, the rated apparent power, and VI constant (seconds) of the jth virtual machine, which is variable and depends on operating states, respectively. N_{SG} and N_{CIG} specify the number of SGs plants and virtual machines, respectively. The reason for the low inertia in the renewable energy source-dominated power grid is that the VI, $H_{CIG,j}$, is small, resulting in significantly reduced effective inertia H_{eq} in the grid.

3. Model-, measurement-, and forecasting-based estimation methods for inertia in renewable power systems

Inadequate inertia in a renewable power system may cause frequency and voltage fluctuations and higher power outage risks. Variable RES poses a risk in balancing supply and demand, as well as frequency control [25]. An unequal inertia distribution affects angular and frequency stability. Monitoring regional inertia and using forecasting tools helps operators adjust generation schedules to maintain sufficient levels of inertia, ensuring reliable integration of renewable sources. Estimating RES inertia requires a longer period of time than that of traditional plants. Synchronous inertia is determined by generator output power changes and ROCOF data during disturbances, while RES inertia analysis requires more data over a longer period [26].

In renewable-rich power systems, the traditional assumption of constant inertia is no longer valid and has been replaced by advanced methods that rely on system measurements and physical modeling. In this context, inertia is increasingly treated as an estimable parameter, determined through parameter estimation and system identification techniques tailored to modern power grids. Three main categories, including model-based, measurement-based, and forecasting-based estimation methods, are proposed according to the time horizon of interest, such as offline post-fault, online real-time, and forecast approaches. Although most model-based methods depend on the swing equation and details of the power system and focus on inertia from SGs, measurement-based methods using PMUs facilitate the consideration of VI due to their variable dynamic behavior. The variability of inertia in RESs arises from several factors, including the reduction in SGs, the intermittent nature of RESs, the reliance on power electronics that lack inherent inertia, differences in dynamic response characteristics, and

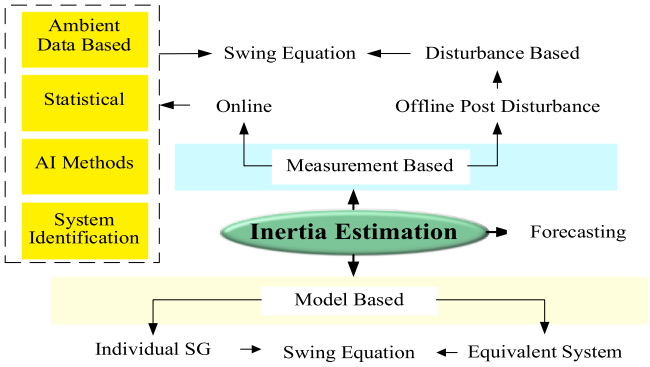

Fig. 1. Inertia estimation classification.

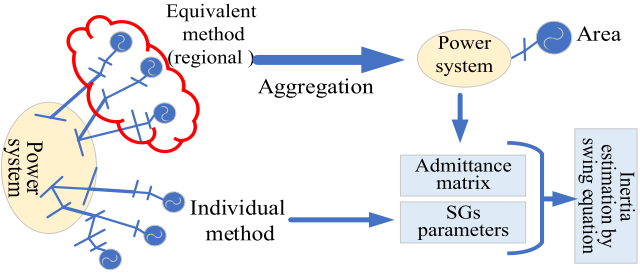

Fig. 2. Structure of model-based inertia estimation method.

regional disparities in the distribution of energy resources. As a result, several key factors must be considered when estimating inertia in renewable power systems. Fig. 1 illustrates these categories and their branches for better identification of subsets.

3.1. Model-based estimation

In model-based inertia estimation approaches that depend on the dynamic representation of SGs, the inertia constant is estimated using the following objective function:

$$min\, j(\theta) = 0.5 \int_0^{T_0} (y_r - y)\, T\, (y_r - y) dt \tag{8}$$

$$\begin{cases} \dot{x} = f(x, u, \theta) \\ y = h(x, \theta) \end{cases} \tag{9}$$

where y_r is the output of the observed system as derived from measurements, y denotes the output of the model, and T_0 represents the duration of the dynamic trajectories of y_r and y [25].

Existing model-based methods have been categorized mainly into two types, including individual SG inertia estimation and equivalent system inertia estimation. Different methods are proposed in Refs. [25,27,28] to determine the parameters of individual SGs. Model-based inertia estimation is adopted in Refs. [29,30], which demands only the network admittance matrix for satisfactory performance. The computational workload of solving differential-algebraic equations with numerous SGs can be reduced by using the dynamic equivalent of coherent SGs to estimate the equivalent inertia of a regional system [31]. The conception of coherent generators is introduced in Refs. [32,33]. Fig. 2 shows the structure of model-based estimate inertia method.

Model-based methods have certain drawbacks, including inaccuracies in the network admittance matrix due to the unavailability or imprecision of detailed system models. Additionally, uncertainties in transmission line and transformer parameters further impact their reliability. It can be challenging to acquire precise information on the line

Table 1
Model-based inertia estimation methods based on the swing equation.

Implementation Method	Pros (✓)/Cons (×)	Formulation	Ref
R approach (accommodates only frequency dynamics)	✓Considered load frequency and PFC ✓Increased accuracy using filtering and curve fitting ✓Applicable at any selected time with symmetric or antisymmetric range × Limited to frequency-based dynamics × Sensitive to noise in frequency measurements	$2H_{est}\frac{df(t_{s+1})}{dt} = R(t_{s+1})\Delta f(t_{s+1}) - \Delta P_{dist}$	[36]
V approach (considers only voltage dynamics behavior)	✓Suitable for systems where voltage control is a priority ✓Lower hardware requirements × Estimation errors increase with different load modeling from the method × Voltage measurements at all load buses may not be available × Method is effective when system loads match a constant current model.	$H_{est} = \frac{\Delta P_L(t) + \Delta P_{dist}}{2\frac{df(t)}{dt}}$	[37]
RV approach (includes both frequency and voltage dynamics in IE and is expected to be more realistic)	✓Various power changes from different sources can be captured × Efficient load models are needed for simulating system behavior during disturbances.	$H_{est} = \frac{R(t_s)\Delta f(t_s) - \Delta P_{LV}(t_s) - \Delta P_{dist}}{2\frac{df(t_s)}{dt}}$	[38]

conductance (G) and susceptance (B) values required to create the admittance matrix ($Y = G + jB$). This data is frequently not readily available or may change with variations in system parameters, making it difficult to establish an exact admittance matrix, particularly in complex systems. Variations in system configuration or unmodeled system dynamics can lead to errors in inertia estimation [34]. Accurately determining the internal reactance of CIGs presents a challenge. The inertia response of Inverter-Based Resources (IBRs) differs fundamentally from traditional synchronous generation. These differences complicate the integration of IBRs into inertia models, resulting in inaccuracies in systems with high RES penetration [35]. These issues are encouraging researchers to use measurement-based approaches. Table 1 compares some model-based approaches and their features.

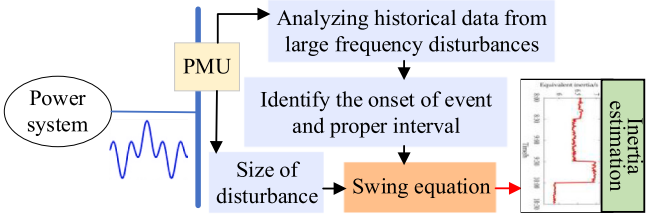

Fig. 3. Structure of offline measurement-based inertia estimation.

3.2. Measurement-based estimation

The measurement-based estimation methods offer advantages over model-based approaches by eliminating the need for complex system modeling [39]. They can estimate inertia for individual generators or the whole system, facilitating targeted control and protection strategies. A major challenge of inertia estimation methods that rely on measurements, especially when using PMUs in power systems, mainly centers around the difficulties in accurately estimating the RoCoF. Below are the main aspects to take into account:

- **Dependency on disturbance:** Most traditional measurement-based inertia estimation techniques depend on large disturbances, such as load shedding or generator tripping events, limiting real-time monitoring. Additionally, identifying suitable disturbances for online estimation poses challenges, making it difficult to accurately assess disturbance size using only frequency data [40].
- **Noise sensitivity:** White noise, which may arise from multiple origins, such as equipment, vibrations, electromagnetic interference, physical disturbances in the transmission lines, communication noise, and temperature changes, affects the quality of PMU measurements. Filtering methods like Kalman or low-pass filters are essential to maintain accurate inertia estimation results despite these influences [41].
- **Utilization of generator terminal bus frequency:** Because of the lack of accessibility to the rotor speed data, generator terminal bus frequency is employed as a representative of the rotor speed. As a result, it may affect the accuracy due to the differences between the terminal bus frequency and the actual rotor speed.
- **Dependency on the number and location of PMUs:** The optimal placement and number of PMUs have a significant effect on the accuracy of estimated inertia, which results from the quality of the collected data [42]. Some methods reduce frequency fluctuations at specific locations by averaging frequency measurements from PMUs [43].
- **Dependency on size of measurement window:** The accuracy of inertia estimation is influenced by the size of the measurement window. Larger windows capture more data but can cause processing delays, while smaller windows may miss important events. With the swing equation method, prediction errors above 10 percent can occur due to the challenge of determining the optimal window size, especially when inertia constants are typically unavailable [44,45].
- **Time synchronization issues:** To accurately calculate inertia, high sampling rates are required, which conventional SCADA systems cannot provide. This can be addressed by sourcing data from the data acquisition system of generators. However, in a large network, the sheer number of generators and the potential lack of time synchronization complicate reliable inertia calculations [40].

The measurement-based estimation methods are categorized into two main groups, which are discussed below.

3.2.1. Offline measurement-based estimation

Offline post-fault inertia estimation methods in power systems involve analyzing data from large frequency-disturbing events to estimate the total inertia of the system. Most of these approaches rely on the swing equation combined with processed PMU measurements to calculate the inertia constant. Although offline methods offer valuable insights for scheduling and planning, they are not suitable for preventing frequency events or ensuring real-time stability [6]. However, challenges arise when estimating inertia in systems with low inertia and high RES penetration. The reliance on historical data from large disturbances limits continuous application, especially in systems with variable inertia levels. Estimating inertia is heavily dependent on major disturbances,

which may not occur frequently, limiting the analysis. [46]. In systems with high-RES penetration and Fast Frequency Regulation (FFR) services, rapid frequency changes make accurate RoCoF calculations difficult and affect the reliability of inertia estimation. Storing accurate data during frequency events may increase accuracy, but reliability depends on system conditions [17]. Fig. 3 depicts the structure of offline measurement-based post fault inertia estimation.

Previously, the inertia in power systems, such as the Nordic [47], Great Britain [48], Western Electricity Coordination Council [11], and Japanese power systems [10], was calculated based on the offline swing equation without considering RES integration. Reference [49] presents a power system inertia estimation method by analyzing power perturbations triggered by the flow switch on an HVDC interconnector. An energy-based estimation method is employed, allowing inertia calculations from non-step power changes while addressing challenges of real data from Ireland's all-island power system. The technique accounts for small frequency deviations, background load-demand variations, PMU measurement noise, and limited system information. In the method, it is needed to consider minor frequency disturbances, background effects on the load–demand balance, noise in PMU data, and the availability of system information. By integrating power over time to compute delivered energy, the proposed method smooths signals. Subsequently, logic is applied to estimate the system frequency.

The main drawback of offline methods is their inability to provide real-time information on inertia before a disturbance. This makes them unsuitable for dynamic operations that require immediate adjustments to maintain stability, particularly in systems with high power-electronics-based generation, such as wind or solar power, which contribute inertia differently than synchronous machines [40]. The primary limitations of post-disturbance measurement-based inertia estimation methods include reduced accuracy due to dynamic system behavior, limited temporal resolution (30–60 min), dependency on system conditions and large disturbances, sensitivity to the location, size, and type of disturbance, lower reliability in the presence of FFR services, and the inability to provide continuous inertia estimation.

3.2.2. *Online measurement-based estimation*

Online or real-time measurement-based methods estimate inertia using PMU measurements of frequency and active power during disturbances, in contrast to post-fault methods, which rely on historical data from significant disturbance events. These real-time approximations could offer closer real-time data regarding the system inertia. Estimating inertia in real time is difficult due to selecting appropriate disturbances and accurately determining their size using PMU measurements [17,20]. Challenges with this estimation method include inaccurate total system inertia estimation, prolonged time needed for inertia estimation, and heavy computational load caused by an extensive dataset. The mentioned offline and online measurement-based inertia estimation methods primarily rely on the swing equation, which incorporates processed PMU measurements of frequency and active power or ambient data, as follows.

a) Swing Equation-based Estimation

The swing equation-based online measurement estimation techniques consist of approaches based on transient frequency and swing equation deformation [50,51]. By tracking the interactions between variations in active power and following frequency variations during regular system operation, inertia is measured using transient frequency methods. In Ref. [52], researchers proposed an online disturbance-based inertia estimation method that improves upon traditional least squares methods by applying weights within the decentralized least squares estimation process. A least squares method using a swing equation is proposed in Ref. [53] to estimate area equivalent inertia based on PMU locations at boundary buses. The result shows that accuracy is good in the first few seconds following a perturbation, but for large-scale systems it decreases and depends on the number and placement of PMUs.

A proposed framework [14] employs PMUs during the transient period following a disturbance, in combination with the estimation of signal parameter via rotational invariance techniques signal processing method, to identify modal parameters. It addresses issues such as phase step errors by deriving an equivalent mode from multiple frequency components. Using an equivalent swing equation to emulate bus dynamics, this approach enables reliable inertia estimation even in systems with a high share of power-electronic-interfaced renewable generation. Nonetheless, its reliance on precise mode identification and the increased computational time for higher model orders can challenge practical real-time application. In Ref. [54], the disturbance onset is detected using the Teager–Kaiser energy operator (TKEO) in the initial stage. This is followed by simultaneous estimation of the RoCoF and active power deviation amplitudes using first- and zero-order O-spline -based differentiators of the discrete-time Taylor–Fourier transform (DTTFT). Finally, the inertia is estimated by evaluating the amplitude of active power deviations and RoCoF via O-splines, with the optimal estimate derived at the center of the 2-s window, 1 s after the disturbance. Although the method is practical, noise and discontinuities in the frequency data can impair the estimation of the RoCoF, which can be mitigated through polynomial fitting and filtering techniques [13,14].

Some methods combine elements of both transient frequency analysis and swing equation deformation to enhance the accuracy and reliability of inertia estimation. For instance, Ref. [55] proposes a numerical-integration-based approach combined with streaming dynamic mode decomposition (sDMD) to estimate both constant and time-varying inertia in non-synchronous devices. The swing equation is reformulated in an integration form to suppress noise and extreme sampling effects, enabling snapshots of power and frequency increments to be constructed. The sDMD then extracts and updates low-dimensional linear operators from consecutive snapshots, reconstructing the integrated swing equation to obtain instantaneous inertia. The method operates without hyperparameter tuning, requires minimal data storage, and demonstrates superior accuracy across diverse device types and control modes. The method in Ref. [56] integrates a low-order system frequency response model with a first-order turbine model. Signal parameters are estimated using rotational invariance techniques. For initial parameter extraction from PMU measurements, a weighted nonlinear least squares approach is used to estimate system parameters such as inertia and the damping coefficient. It still needs a lengthy period of data and complex processes. Furthermore, inadequate generalizability might arise from transfer function approximations that are completely basic. RES integration causes rapid changes in power system inertia and challenges accurate estimation during large disturbances at different time intervals. To address this issue, inertia levels should be continuously estimated during normal operation, which allows TSOs to provide corrective solutions quickly and sustain a resilient and stable system [57].

b) Ambient Data-based Estimation

Real-time inertia estimation using existing approaches faces challenges because it requires extracting oscillation modes from historical PMU data following a disturbance. On the other hand, these oscillation modes can be identified using PMU ambient data, which is a constant feature of the power system, even in the absence of disturbances. Ambient data captures natural, low-level fluctuations in the power system, including power and frequency variations measured in real time [58,59], as well as bus voltages and line currents [60]. These fluctuations arise from random load changes or minor disturbances, excluding significant events like faults or major outages. Inertia can be effectively tracked through ambient measurements not only to post-frequency disturbances but also while the system is operating normally. Therefore, the TSOs can calculate the amount of time they have to implement

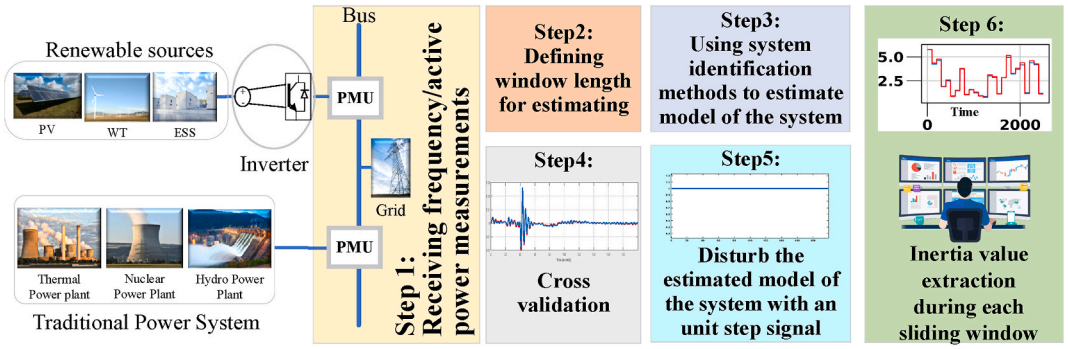

Fig. 4. Structure of online measurement inertia estimation.

frequency response before surpassing allowed frequency limits and experiencing power outages or additional disturbances. This indicates that the fast-acting reserve amount can be determined and assigned for each region of the power grid, with specified response time criteria [61,62].

System identification methods such as state-space models [44,63], transfer functions [64], auto-regressive moving average exogenous (ARMAX) model [61], grey box transfer function model [65], and Iterative Equation Error model [66] are used to estimate the system model using data from PMUs as inputs and outputs. Fig. 4 shows the structure of online measurement inertia estimation. These methods require a proper data window length to accurately estimate the system model and extract the inertia value.

Several researchers have conducted research on inertia estimation methods based on ambient data. The inertia constant, as defined by the oscillation modes, is derived from the transfer function representing the oscillatory characteristics of a generator operating under normal excitation circumstances:

$$H = K_0\left(1-\zeta^2\right)f_d^{-2} \tag{10}$$

$$K_0 = \omega_0\, P_{e0}\, \cot\delta_0 \;/\; \left(8\pi^2\right) \tag{11}$$

where K_0 is the steady-state coefficient, P_{e0} is the steady-state electrical power, ω_0 is the rated rotor speed, δ_0 is the steady-state rotor angle, and f_d and ζ are the oscillation frequency and damping ratio, respectively.

Once the synchronized ambient data reveals the oscillation modes, the inertia can be estimated based on directly measured or calculated steady-state variables P_{e0} and δ_0 by a PMU [32]. An online estimation method is developed in Ref. [62] to calculate the effective inertia of regional power areas, but it is limited to an equivalent two-machine system. This method adopts the values of inter-area oscillation modes derived from ambient data on voltage and current at the boundary buses connected to the critical cut set. The aggregated SG power angle δ_{ASG_i} is estimated, and the modes are extracted from the measured ambient data of the frequency of each area. After determining the mathematical relationship between H_{ASG_1} and H_{ASG_2} based on the derived modal information, the equivalent inertia using the equivalent power angle, modal frequency, and damping extracted. Finally, the effective inertia of the relative area is calculated from:

$$H_{eff} = \frac{H_{ASG_1}\cdot H_{ASG_2}}{H_{ASG_1}+H_{ASG_2}} \tag{12}$$

where H_{ASG_1} and H_{ASG_2} are the estimated inertia constants of the area 1 and area 2, respectively, in seconds. The covariance matrix of ambient measurements is proposed in Ref. [60] to align data with traditional SG modeling, allowing the estimation of both real inertia from SGs and VI from converter controllers. This mimics synchronous machines and predicts grid-following converters droop, emulating swing equation damping. Nevertheless, an optimal strategy is essential for identifying the placement of PMUs to gather ambient data. The ability of the method to withstand imperfect measurements and the impact of errors have not been addressed. In Ref. [57], an inertia estimation method is proposed for the Japanese power system, using PMU background signals without needing prior knowledge of RoCoF, disturbance sizes, and load/RES conditions on both the generation and demand sides. This method utilizes the background signals of PMUs through three key factors: the extracted proportions of the frequency response, inter-area oscillation, and synchronizing power based on small-signal stability. However, this method does not apply to VI from CIG.

A key challenge in leveraging continuous ambient data for real-time inertia estimation lies in detecting the subtle frequency deviations caused by minor power imbalances. These deviations are often smaller than the background oscillations inherent in the system, making it difficult to reliably distinguish them as true inertia-related frequency responses [40]. Tables 2 and 3 provide a summary of the model types, investigated techniques, and pros, as well as cons of the previously mentioned model-based and offline and online measurement-based

Table 2
Offline post disturbance measurement-based inertia estimation methods.

Implementation Methods	Area	Pros (✓)/Cons (×)	Formulation	Ref.
A modified Detrended Fluctuation Analysis identifies event type and start time, with inertia estimation via RoCoF in a 500 ms sliding window.	T	✓Robustness to non-stationary data × Dependency on the location of PMUs, the time and size of Disturbance, and the system loading conditions × based on the simplified swing equation × neglecting the impact of load frequency, voltage dependency, and the SGs control loops	$\frac{df}{dt} = \frac{\Delta P}{2H}{}^{*}f_0$	[71]
Using the frequency spectrum to analyze the RoCoF calculations from PMUs over 500 ms and applying the equivalent swing equation	R	✓Improving accuracy in detecting disturbances × Regional estimation methods are inadequate for accurately estimating the COI frequency × The impact of PSS has not been evaluated.	$M_j = \frac{\Delta P_j\left(f_{sj}\right)}{\frac{df_j}{dt}}\sim\Delta M_j$	[72]

Note that: T is Total and R is Regional.
$M_j = 2\,H_jS_j$, where M_j is the angular momentum (MWs), H_j and S_j are the inertia constant and the total generated power of an area j.

Table 3
Online measurement-based inertia estimation methods.

Implementation Methods	Area	Pros (✓)/Cons (×)	Formulation	Ref.
Estimation based extended Kalman filter using swing equation	T	✓Effectively handle non-linearities ✓Sensitivity analysis × The method is more sensitive to time of disturbance × RESs VI effects have not been considered × Voltage and frequency control systems have not been considered × Dependency on disturbance	$\hat{x}_k^- = f(\hat{x}_{k-1}^-, u_k, 0) = \begin{pmatrix} \delta_{k-1} + (\omega_{k-1} - \omega_0)\omega_B \Delta t \\ \omega_{k-1} + \frac{\Delta t}{2H}\left[\frac{EV_k}{X_d} sin(\delta_{k-1} - \theta_{k-1}) - D(\omega_{k-1} - \omega_0)\right] \\ H_{k-1} \end{pmatrix}$	[73]
Sliding window inertia estimation based on swing equation	R	✓Robust against measurement noise ✓Reduces false detections × Dependency on disturbance onset × Loss of precision due to inherent phase-step error	$H = \frac{0.5(P_1 - P_2)}{(R_2 - R_1)}$	[74]
Using ARMAX	I	✓Estimates inertia from ambient data × the inertia tracking trajectory could not be provided in real-time × only synchronous units have been considered	$M_{Sk} = -\frac{\sum_{i=0}^{N} 1/h_{ii}(0)}{\sum_{i=0}^{N} h_{ki}(0)/h_{ii}(0)}$	[61]
Using the simplified first-order ARMAX applied to Ambient data	T	✓Independence of RES penetration level × Efficiency depends on disturbance location × Dependency of window length on the number of areas, adopted control systems, and noise level	$H = -\frac{1}{2B_r}$	[75]
ARMAX model	I	✓Robust to noise ✓Low computational complexity × Disturbance onset is needed to isolate the inertia response of SG from other dynamics.	$H = -\frac{1}{2B_r}$	[76]
Closed-loop micro-perturbation method (MPM)	T	✓Handles time-varying inertia × Precise estimation requires well-designed probing signals, complicating implementation × High detection signals are needed for a reliable signal-to-noise ratio, impacting system security × Micro perturbations disrupt frequency response	$\Delta\omega = \frac{1}{2H_s + D}(\Delta P_m - \Delta P_e)$	[64]
Adoption of inter-area oscillation mode values from ambient data	R	✓RoCoF and total active power deficit, which are difficult to obtain in practice, are unnecessary in the suggested model × Inter-area oscillation not always present	$H_{ASGi} = -R_e\left\{\frac{\lambda D_{ASGi}\varphi_{\delta i} + \sum_j K_{sij}\varphi_{\delta i}}{\lambda^2 \varphi_{\delta i}}\right\}$	[62]
An ambient modal approach, based on the frequency and damping ratio modes	I	✓Using ambient data to estimate online inertia under normal conditions × Accuracy issues due to measurement errors × Not reliable for online estimation with a long execution time for large network models.	$H = K_0(1-\xi^2)f_d^{-2}\ k_0 = \omega_0 Pe_0 \cot\delta_0 / (8\pi^2)$	[32]
Decentralized data-driven inertia estimation using an Adaptive Unscented Kalman Filter	I	✓Prevent communication failure in the decentralized method × Method limited to SGs, unable to extract useful info from ambient measurements	$\omega_k - \omega_{k-1} = \frac{\omega_s \Delta t}{2H_{k-1}} \times \left(P_{e0} - \frac{E'_{k-1} V_{t,k}}{x'_{eq}} \sin(\alpha_k - \theta_k)\right)$	[28]

Note that: I is Individual.
P_1, P_2, R_1, R_2 are four smoothing filters applied as sliding data windows, where P represents active power and R denotes the frequency derivative. Subscripts denote the first and second windows.
M_{Sk} is the system inertia, N is the number of total areas, $h_{ki}(0)$ is the response of the ith output of the MIMO.
system at time t = 0 to a unit impulse in the kth input, the sum of $1/h_{ii}(0)$ value corresponds to the system COI frequency.
B_r is the numerator coefficient of the first-order reduced continuous-time transfer function; it has units of seconds and is numerically equal to the inertia constant H.
$K_s = \frac{\partial P_e}{\partial \delta}$ is the matrix of synchronizing power coefficients, φ_δ is the angles mode shapes, D_{ASG} is the damping coefficient of the aggregated synchronous generators, and λ is the eigenvalue of the system state matrix.

estimation methods.

c) Artificial Intelligent-based Estimation

Progress in PMU-based wide-area measurement systems has made data-driven methodologies a viable alternative to traditional approaches [67]. These methods possess notable features like learning and predictive capabilities, effectively mapping the relationships between power system parameters (input) and inertia estimation (output). Innovative Machine Learning (ML) approaches, such as the Long Short-Term Memory Recurrent Convolutional Neural Network (LRCN) and Graph Convolutional Network (GCN) [9], utilize ambient data from optimal

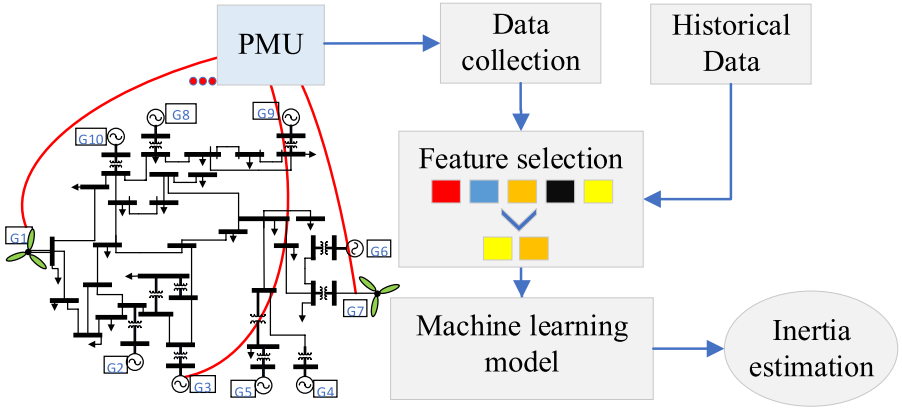

Fig. 5. Structure of online inertia estimation based on ML method.

Table 4
Inertia estimation based on ML methods.

Methods	Key Features	Advantages	Disadvantages	Ref
LRCN & GCN	Utilization of LRCN for temporal behavior of time-series data processing and GCN for spatial data analysis from multi-node PMUs.	Efficient mapping of system parameters to inertia estimates.	Difficulty in capturing long-range spatial relationships in GCNs due to data diffusion across layers	[9]
Q-learning & Ambient Data	Continuous inertia estimation under ambient conditions, using Q-learning to analyze mechanical power fluctuations and correct inaccurate estimates.	It does not need a separate training phase, that is useful for online applications.	Does not account for VI.	[25]
DNN-Based Inertia Estimation	Estimation of minimum inertia demand based on frequency security constraints like RoCoF and maximum frequency deviation by using offline trained DNN.	Can map non-linear relationships in the system.	Requires extensive offline training data and may be limited by the operational state of the system.	[68]
CNN for Inertia Estimation	Use of spectral analysis of voltage measurements from IBR-dominated grids to continuously estimate inertia.	Automatic feature selection, no need for manual feature extraction.	Limited ability to generalize across different configurations and lack of transparency in predictions.	[69]

Table 5
Summary of ML-based inertia estimation methods and their validation scope.

ML Methods	Real-world Data Used?	Accuracy	Limitations/Disadvantages	Ref
Switching Markov Gaussian Model (Unsupervised ML)	Yes - 2 consecutive years of UK PMU historical data (half-hourly avg) (Ambient data)	Minimizing mean squared error (MSE) $<$ 0.1 $s2$ for 95 % of daily estimates; robust to up to ~2 h data loss	SMGM is valid for real-time inertia estimation only in normal conditions; the historical dispatch information is only available at 5 min Intervals; it does not consider CIG or load-side inertia.	[43]
LRCN (temporal) + GCN (spatial)	No — IEEE 24-bus system (Ambient data)	Achieved ~97–98 % accuracy in simulations	No validation on real PMU data; sensitive to features extracted and number of PMUs; it does not consider CIG or load-side inertia	[9]
CNN + spectral analysis	No — IEEE 39-bus comprising SGs, static compensators and CIG (Ambient data)	Mean absolute percentage error equal to 1.79 %	No field PMU validation; only synthetic testing; it does not consider CIG or load-side inertia	[69]
Q-learning RL + energy variations	No - IEEE 39-bus (Ambient data)	Prediction errors of less than 10 %	No validation on real PMU data; it does not consider CIG or load-side inertia.	[25]
Multi-head GAT	No — IEEE 24-bus system (Probing signal)	The presented model achieved 15.63 % and 31.7 % in MSE compared with GCN with/without considering noise	No real PMU usage; it does not consider CIG or load-side inertia.	[77]
Residual neural network (ResNet)	No — IEEE 39-bus (Disturbance)	Absolute prediction errors of less than 5 %	Small datasets; no real PMU usage; it does not consider CIG or load-side inertia.	[78]
Dual-stage hybrid deep learning method combined with hybrid networks	No - IEEE 39-bus + IEEE 68-bus system (Ambient, disturbance)	Average MSE is less than 3.5 %	No real PMU usage; it does not consider CIG or load-side inertia.	[79]
Multivariate Random Forest Regression (MRFR)	Partial — ERCOT 6102-bus power system + U.S. WECC system + CURENT Hardware Testbed (Ambient data)	Absolute prediction errors of less than 5 %	Limited real-world deployment; it does not consider load-side inertia	[80]
MRFR	FNET/GridEye measurements and the WECC system (Ambient data)	The average and maximum error is lower than 4 % and 9 %, respectively.	It does not consider CIG or load-side inertia.	[67]

multi-node PMUs to enhance inertia estimation. Additionally, a wrapper feature selection algorithm improves feature combination efficacy. In Ref. [25], a method for continuous online inertia estimation uses changes in electrical and kinetic energy influenced by control systems like governors, which are explored through the Q-learning technique. A Deep Neural Network (DNN)-based approach in Ref. [68] estimates minimum inertia demand while considering frequency security constraints such as RoCoF and maximum frequency deviation, using operational state parameters as offline training data. The authors in Ref. [69] apply a Convolutional Neural Network (CNN) and utilize spectral analysis of voltage measurements to optimize frequency bands without manual feature selection, highlighting the importance of accurate input feature selection to prevent bias and errors [70]. Fig. 5 illustrates the structure of online inertia estimation using ML methods.

Moreover, neglecting to account for operating conditions across specific frequency bands in the training set can lead to inaccurate predictions, particularly when new devices are integrated into the system. Table 4 summarizes the key ML-based approaches for inertia estimation, highlighting their strengths and limitations in handling the complexities of modern power systems, particularly those with high renewable energy integration.

Recent advances in ML techniques have shown tremendous potential towards power system inertia estimation. Nevertheless, there is limited extensive practical verification using real operational data. To provide some illumination to this issue, the current research incorporated a focused literature review to present an overview of prominent ML-based inertia estimation approaches and indicate their validation procedures and datasets. Table 5 presents a comparative summary of these methods, classified by validation type: real PMU measurements, hardware-in-the-loop tests, or simulation records only. The summary highlights the disparity between mathematical developments and practical deployments, underlining the need for greater real-data validation in current research.

Table 5 provides a concise overview of some of the recent ML-based inertia estimation methods, describing their key algorithmic approach, input parameters, and testing ranges. A distinction is made between methods validated solely on simulated data, those tested against small-scale PMU records, and the few compared with actual operational records. In practice, this summary benefits both system operators and researchers by clearly indicating which ML methods have reached the deployment stage and which remain at the proof-of-concept phase. Notably, although some approaches (e.g., Switching Markov Gaussian Models optimized for the UK grid [43]) have achieved low estimation errors for specific applications, most methods are still required to be validated across a broad set of operating conditions. This highlights the necessity for more work towards large-scale field testing using actual PMU data.

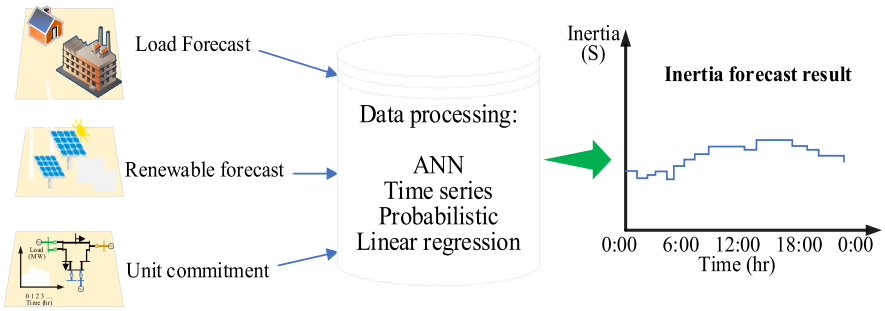

Fig. 6. Structure of forecasting inertia.

3.3. Forecasting-based estimation

Given the immediate and transient character of the inertia reaction, system operators must quickly address inadequate levels of the system inertia response to avoid major losses. In order to secure an adequate supply of fast frequency reserves, adjust the system inertia level in an appropriate proportion, or mitigate the potential for the largest loss, it is essential that the system operators have a precise estimation of the inertia that will be available in the future. This estimate assists them in the planning for necessary reserves and operation of power systems [6, 51]. Within periods of low load, forecasting kinetic energy could play an important role in determining whether the system has sufficient spinning mass for the upcoming operational period. During these periods, real-time estimation could be a vital tool for managing unanticipated events. Consequently, the potential to predict the system kinetic energy should be explored [81].

A number of prediction models, including time series models, probabilistic inertia forecasting models, linear regression models, and models based on Artificial Neural Networks [82–84], have been developed for the purpose of forecasting inertia. The input data required for inertia forecasting includes forecasted load, renewable energy availability predictions, and the operational status of generating units (on/off) within the unit commitment schedule. Fig. 6 shows the main process of forecasting inertia for the day ahead.

However, due to the dynamically changing nature of the contemporary electrical grid, these methods of estimating inertia are continuously evolving. Forecasting inertia in ERCOT is based on physical models using the online status of generators in transmission as follows [15,83]:

$$E_t^{I,G} = \sum_i H_i . P_i^{G,C} . K_{i,t} \tag{13}$$

where i is the number of generators, $K_{i,t}$ is the status of generator in time of t, $P_i^{G,C}$ represents the generating capacity, and H_i is the inertia constant. However, TSOs do not always have access to the expected states of generators prior to real-time operation. The statuses can be influenced by energy markets such as day-ahead and intraday markets, as well as generator bids and expected energy demand. Some factors that affect inertia forecasting present the challenges [84,85], including weather-dependent RESs generation, load variability, generator failures, maintenance schedules, market forces, and strategic behavior of generators.

Table 6
Summary of the contributions of load inertia constants.

Category	$H_{\text{load},P_{dem},district}$ (s)	$H_{\text{load},S_{gen},district}$ (s)
Private households	0.74–4.24	0.05–0.19
Retail businesses	0.09	0.01
Trade, commerce businesses and industry	0.44–0.66	0.05–0.15
Industry	0.51	0.17

3.4. Inertia contribution of the demand side

Unlike the generation side, the demand side has historically been passive, merely consuming electricity. However, recent advancements suggest it can play an active role in grid stability, including inertia provision. Authors in Ref. [86] evaluate the contribution of the demand side to system inertia in the Great Britain power system using historical frequency outage data. By isolating the generation contribution and utilizing the power/frequency ratio (K) as an indicator of additional inertia from spinning reserve, the study reveals that the demand side contributes an average inertia constant of 1.75 s, representing 20 % of the total system inertia (E_{sys}). The demand side inertia (E_{dem}) is estimated by subtracting the generation side inertia (E_{gen}) from the total system inertia ($E_{dem} = E_{sys} - E_{gen}$). The generation inertia is further refined by considering a correction factor (αK) based on the power/-frequency ratio ($E_{gen} = E_{gen,output} + \alpha K$). This demand-side inertia, primarily supplied by synchronous and asynchronous (induction) motors in industrial and commercial loads, and is becoming increasingly non-supportive in low-inertia power systems with the growing use of variable frequency drives, which disconnect motors and reduce their inertial response. Understanding and quantifying demand-side inertia is crucial for future frequency control and the potential development of inertia markets, especially with the increasing penetration of non-inertia providing renewable energy sources. For a real case (Flensburg blackout), the range of the inertia constant is determined by categorizing power consumers into private households, retail businesses, commerce and industry businesses (the categories have been done by the German Association of Energy and Water Industries and transformer stations location) based on calculations that use power demand and apparent generator power [87].

The total inertia in formulation (7) can be extended as in (14), including the contribution of load inertia [87]:

$$H_{sys} = \frac{\sum H_{gen,i} \cdot S_{gen,i}}{\sum S_{gen}} + \frac{\sum H_{load,i} \cdot S_{load,i}}{\sum S_{load}} \tag{14}$$

To calculate the inertia constant of loads in a power system when their apparent power is unknown, two methods are proposed in Ref. [87]. The first approach computes the load inertia constant H_{load,P_dem} using the overall system demand, as given in Equation (15), and applies this to district-level calculations with the kinetic energy of the district $E_{\text{kin,district}}$ and demand $P_{\text{dem,district}}$. The second method derives the load inertia constant H_{load,S_gen} by leveraging the total apparent power of all connected synchronous generators, as shown in Equation (16), and can also be used per district with the kinetic energy of district $E_{\text{kin,district}}$ and the apparent power generators S_{gen}. This latter method provides a clearer view of the power consumers' inertia contribution to the total system inertia.

$$H_{\text{load},P_{\text{dem}}} = \frac{E_{\text{kin,load}}}{P_{\text{dem}}} \tag{15}$$

$$H_{\text{load},S_{\text{gen}}} = \frac{E_{\text{kin,load}}}{S_{\text{gen}}} \tag{16}$$

The total kinetic energy contributed by power consumers accounts for 21.21 % of the total stored kinetic energy in the system. Table 6 shows the inertia contribution per district from each power consumer category, calculated using formulations (15) and (16), with the maximum inertia constant observed in private households.

Ref [88] investigates and quantifies the potential for virtual inertia from the load side using voltage-dependent loads integrated with electric spring (ES) technology in an isolated microgrid scenario with CIGRE European benchmark. The analysis demonstrates that these smart loads (SL), operating within a ±5 % voltage tolerance, can effectively provide virtual inertia. According to U.K. National Grid frequency requirements, the ES-based impedance type smart load can achieve an inertia coefficient of up to 2.5 s (for power exponent np = 2) relative to their load power rating. Inertia values peak during winter nights due to electric heating demand, and reach their lowest in summer when domestic power consumption and power-voltage sensitivity are low. For most of the day, smart loads can supply about 1.3 s of additional virtual inertia.

Accurate estimation of load inertia is crucial for assessing its contribution to system stability. Recent methodologies include using ambient measurements from synchrophasor technology, which allows for real-time monitoring time-varying inertia of the composite load model of WECC without requiring disturbances [89].

3.4.1. Inertia contribution of the electric vehicles (EVs)

In recent years, EVs have been increasingly integrated into power systems as flexible loads to support the balance between generation and demand [90]. While unmanaged EV charging can exacerbate frequency deviations, EVs equipped with bidirectional chargers under V2G technology [91], EVs are capable of rapidly injecting or absorbing excess power, offering significant potential for enhancing frequency regulation and overall system stability [92]. By applying virtual synchronous machine (VSM) or VSG control through the AC/DC bidirectional converter, EVs can emulate virtual inertia, damping, and excitation characteristics, allowing them to serve as flexible buffers between the grid and the vehicles. This approach supports frequency regulation, mitigates rapid frequency fluctuations, and enhances dynamic stability, while also reducing the negative impact on EV charging during sudden frequency disturbances [90,93,94]. In Ref. [94], frequency stability in isolated grids with high renewable energy penetration is improved by integrating VSM control into EV charging infrastructure, including charging stations (CSs) and battery swapping stations (BSS), enabling EVs to actively contribute to grid frequency regulation. It introduces a two-stage frequency regulation strategy: a day-ahead scheduling model that optimizes generation and EV dispatch to reduce costs, and a real-time control stage that uses a consensus algorithm to dynamically allocate power adjustments among participating units in response to real-time frequency deviations, enabling rapid and coordinated actions to maintain system stability. The formulation for VSM inertia is given as follows:

$$J\frac{d\omega}{dt} = \frac{P_m - P_e}{\omega} - D(\omega - \omega_g) \quad \frac{\mathrm{d}\delta}{dt} = \omega - \omega_g \tag{17}$$

where J represents the rotational inertia D denotes the damping coefficient. ω refers to the virtual angular frequency, which remains close to ω_0 because frequency fluctuations are relatively small. ω_g denotes the measured angular frequency. The mechanical and electromagnetic power for the converter can be considered as:

$$P_m = P_{ref} - K_f(\omega_0 - \omega_g) \; P_e = \frac{E - V_g}{X_f}\delta \tag{18}$$

where P_{ref}, E, and V_g represent the rated power of the VSM, and the voltages of the converter and the point of common coupling, respectively. K_f denotes the droop coefficient of the primary frequency control. The presence of the filter circuit introduces a line impedance, X_f, which corresponds to the reactance of the filter. δ is the power angle difference between the VSM and the power system, which is small [94]. An adaptive virtual inertia in multiple CSs for inertia supporting power is proposed in Ref. [95]. The initial inertia value $J_{i,0}$ of CS VSG is:

$$J_{i,0}^2 = 4\Gamma_i(D_i\Delta\omega_i - \Delta T_i) \tag{19}$$

$$\Gamma_i = k_s\Delta\omega_i + k_a\sum_{j=1}^{n} a_{ij}\Delta\omega_{ij} \tag{20}$$

where Γ_i represents the adaptive virtual inertia component, D_i is the virtual damping coefficient, $\Delta\omega_i$ is frequency deviation, ΔT_i is the electromagnetic torque imbalance, k_s and k_a are the adaptive adjustment factors associated with the adaptive virtual inertia, $\Delta\omega_{ij}$ is the frequency deviation between neighboring CS VSGs, and the index i denotes i-th CS VSG. A synthetic inertia power-sharing method using V2G and bidirectional EV chargers is represented in Ref. [96] to mitigate the dynamic effects of high RES penetration and non-synchronous generators. The formulation for emulated synthetic inertia is defined as follows:

$$\Delta P_{EV\_syn} = \frac{J_{sys}.s + D_{syn}}{1 + T_I}.\Delta f \tag{21}$$

where J_{sys} and D_{syn} are two parameters of the virtual rotor component: the synthetic inertia constant (s) and the synthetic damping constant (s), respectively. T_I is the time constant of an inverter unit (s), Δf is the frequency deviation of the system (Hz), and ΔP_{EV_syn} denotes the change of synthetic inertia power from V2G system (p.u.). Accurate real-time estimation of virtual inertia enables EVs equipped with bidirectional charging and participating in V2G to dynamically adjust their response, optimize power exchange, and provide timely frequency support. This capability not only enhances grid stability but also ensures efficient utilization of EV battery resources while meeting user charging requirements.

4. Practicality and implementation for inertia estimation

Many projects conducted by research institutes or TSOs have worked on inertia estimation and monitoring in recent years, such as EPRI, NREL, NERC, ORNL, ENTSO-E, POSOCO, ARENA, and NESO [15,34,35,40,97–101]. The methods they used are explained as follows.

A. National Renewable Energy Laboratory (NREL)

A novel multivariate linear regression method is proposed in Ref. [34] for real-time inertia and frequency response estimation using probing signals. The advantage of this method is its ability to estimate inertia in real-time, even with high levels of IBRs, which traditionally reduce system inertia. By integrating the probing signal with a multivariate regression model, the method accounts for multiple frequency response mechanisms acting within the same time frame. While the approach is effective in dynamic systems, its accuracy depends heavily on the quality of the probing signals and the system response characteristics, which may vary with changing grid conditions. For modeling of IBR frequency response, P_m has not been considered constant in Eq. (2) due to the fast frequency control of GFM and is modeled as follows:

$$P_m(t) = P_m(0) - \frac{K}{2\pi}[\omega(t) - \omega(0)] \tag{22}$$

where K demonstrates the aggregated droop constant in the inertial time interval, $P_m(0) = P_e(0) + D.\omega(0)$, and $\Delta\omega(t) = \omega(t) - \omega(0)$. To reduce the effect of noise measurement, the following equation is derived:

$$2H\frac{S_n}{\omega_n}\Delta w(t) + \frac{K}{2\pi}\int_0^T \Delta w(t)\,dt + \int_0^T \Delta P_e(t)dt = 0 \tag{23}$$

where T indicates the inertial response during measuring data. A probing signal-based with 1-MW Hann signal during is injected into the power system through an inverter to estimate inertia:

$$P_{probe}(t) = \begin{cases} cos^2\left(\frac{t-1}{2}\pi\right) & 0 \le t \le 2 \\ 0 \quad else \end{cases} \tag{24}$$

where P_e is equal to $-P_{probe}$ during the probing signal injection. The probing signal method showed a high correlation with actual system inertia values, with an error margin ranging from 1 % to 5 % under stable conditions.

B. North American Electric Reliability Corporation (NERC)

The four-stage method for determining and managing system inertia, as proposed by NERC [101], begins with calculating the minimum synchronous inertia for a given hour in a year by summing the individual inertia values of all online generators. This inertia is then assessed for its adequacy to handle contingencies, with the RoCoF calculated based on the system loss of generation/load and minimum kinetic energy. The formula for RoCoF without a load damping constant (D) is:

$$RoCoF = \frac{\Delta P_{MW}}{2.K_{E_{min}}}.60\ Hz \Big/ s \tag{25}$$

where ΔP_{MW} represents the loss of generation/load and $K_{E_{min}}$ is the minimum kinetic energy. For systems where load damping constant is available, RoCoF is modified as:

$$\Delta f_{0.5} = \frac{\Delta P_{MW}}{D.P_{load}}\left(1 - e^{\left(-\frac{0.5+D.\ P_{load}}{2.KE(t)}\right)}\right) \tag{26}$$

Stage 2 involves verifying the actual lowest achievable inertia from sources like must-run units and nuclear plants, ensuring it meets or exceeds the minimum inertia obtained from Stage 1. Stage 3 tracks system inertia trends, forecasting the future based on historical data, which emphasizes continuous monitoring when the system operates near minimum inertia. Stage 4 offers mitigation strategies such as bringing additional SGs online, including inertia as a constraint in the unit commitment framework, installing synchronous condensers, and utilizing synthetic inertia from wind turbines to prevent issues related to low system inertia.

C. Australian Renewable Energy Agency (ARENA)

This report, presented in Refs. [97,98], details the use of extensible measurement units (XMUs) deployed across various regions to capture inertia data. The method involves injecting modulation signals from a battery energy storage system (BESS) into the grid and analyzing the system response to estimate total and regional inertia. The focus is on the discrepancies between theoretical and measured inertia values and the operational value of measuring inertia using real-time data with a confidence range of approximately 10 %, a significant improvement over traditional theoretical or event-based estimation methods. During the testing period from June to September 2023, a total of 1078 measurements were collected, and the results showed that the measured system inertia was, on average, 38 % higher than AEMO theoretical estimates. The measured inertia exhibited significant variability, with an upper bound that was 14.2 % higher and a lower bound 10.9 % lower than the actual measurements, suggesting a relatively accurate estimation process with some fluctuations. However, the reliance of the method on the deployment of multiple XMUs and the continuous monitoring required may involve significant infrastructure costs. Furthermore, the measurement is sensitive to the quality of real-time frequency data, and in regions with low renewable penetration or less demand, the system inertia contributions may be more difficult to measure with precision.

D. Power System Operation Corporation (POSOCO)

The online inertia estimation method adopted by the National Load Dispatch Centre in India [40] begins by collecting generator ratings and their inertia constants as input. It initializes a counter to assess each generator's output and circuit breaker status. Generators producing over 10 MW with closed breakers have their kinetic energy estimated based on inertia and MW rating. Those with lower outputs or open breakers contribute no inertia. The total system inertia is calculated by summing the kinetic energies of all active generators. This estimated inertia is then validated against values obtained from frequency disturbances, leading to potential adjustments in online estimation. The approach facilitates continuous real-time monitoring of system inertia, which is essential for grid stability management and is fairly easy to implement due to its reliance on existing SCADA data. However, assuming similar inertia constants for generators lacking data may cause inaccuracies, particularly if their designs or operations vary significantly. The accuracy of the method relies on frequency disturbances; rare or minor disturbances may lead to less accurate system inertia estimates.

E. European Network of Transmission System Operators for Electricity (ENTSO-E)

The ENTSO-E in Refs. [15,35] emphasizes simulation-based methods for estimating the future kinetic energy of generators that are synchronously coupled to the system, either by using output power exceeding a threshold value or circuit breaker position as an indicator. Nevertheless, the impact of load inertia is disregarded in this assessment. This report explores inertia estimation using frequency deviations from specific locations, such as the center of inertia (COI). The advantage of using the COI for inertia estimation is that it provides a centralized measure of system frequency, making it useful for large, interconnected grids. Nonetheless, accurately determining the COI frequency can be challenging because frequency readings from all the preferred locations might not be accessible. A simulation model was used to assess kinetic energy variations under different future scenarios (2020 and 2025). This model incorporates factors such as market simulations, varying RES infeed, and HVDC links, which influence the system inertia levels. The model is designed to provide short-term forecasts and real-time assessments of system inertia, facilitating better planning and operational responses. The main advantage of these methods is their adaptability to different system conditions, including the integration of synthetic inertia. However, their reliance on simulation models can limit their accuracy in real-time applications, particularly when forecasting long-term system behavior under changing generation mixes.

5. Implementation challenges for real-time inertia estimation tools

Integrating real-time inertia estimation into grid operations involves more than just creating accurate algorithms; it also requires addressing several technical, operational, and institutional challenges. Weaknesses in measurement and communication systems, increased exposure to cyber-attacks, and strict regulations all add to the difficulty. Incomplete observability caused by the limited number of PMUs further reduces the reliability of estimation. Together, these issues reveal a clear gap between ongoing research and its practical application in control centers.

- Data Latency and Synchronization

PMUs generally provide measurements at 30–60 samples per second, much more quickly than traditional SCADA systems. End-to-end latency from PMU to control-room processing tends to vary from tens of

Table 7
Implementation challenges for real-time inertia estimation.

Challenges	Causes	Impact on Inertia Estimation	Mitigation Strategies
Data Latency and Synchronization	Network delays, data aggregation, legacy control room hardware, complex precise time coordination	Delayed system response to fast frequency changes, reduced estimation accuracy and reliability	Design low-latency architecture, use edge computing, improve time synchronization, upgrade communication infrastructure
Cybersecurity Vulnerabilities	GPS spoofing attacks, false data injection (FDI), man-in-the-middle (MITM) attacks, lack of multi-layered security frameworks	Incorrect inertia estimation, risk of improper grid control, reduced operator trust	Data encryption, network segmentation, anomaly detection, secure time synchronization protocols
Regulatory and Policy Framework Constraints	Existing regulations not covering new tools, organizational resistance, operator training requirements	Slow adoption process, incompatibility with operational and market standards	Update regulations and standards, provide operator training, engage continuously with regulatory bodies
Computational Scalability and Hardware Constraints	Heavy ML models, outdated and low-performance hardware, lack of model optimization	Delays in estimation execution, inability to process real-time data effectively	Upgrade hardware with GPUs and advanced processors, model compression, distributed computing
Adaptability to Evolving Grid Conditions	Continuous changes in energy sources, load profiles, and grid topology, static offline-trained models	Reduced estimation accuracy under new conditions, loss of operator confidence	Online and incremental learning, drift detection, scheduled model retraining
Incomplete System Observability and PMU Placement	Economic and logistical constraints in PMU deployment, uneven distribution, insufficient measurement points	Lower accuracy and reliability during critical disturbances	Optimal PMU placement, coordinated installation planning, cost-effective PMU coverage expansion

milliseconds to even some seconds due to network delay and data aggregation behavior, such as waiting for outlier packets prior to releasing synchronized data [102,103]. For real-time inertia estimation to be effective, especially in the case of high-rate frequency control, such latencies can be detrimental to responsiveness and accuracy. Although existing methods allow for sub-microsecond latency measurement in testbeds [104], applying such solutions to operational control center networks requires specialized communications hardware and careful co-design of latency-aware data pipelines.

- Cybersecurity Vulnerabilities

Utilization of PMU data for real-time inertia estimation makes us vulnerable to cyber-attacks through time-synchronization attacks (TSAs) and false data injections (FDI). TSAs such as GPS spoofing have the potential to alter the timing of PMU measurements, resulting in significant estimation errors, without being detected by traditional bad data detection methods [105]. Additionally, low-inertia high--penetration power systems that include inverter-based resources present ever more vulnerable targets for stealthy cyber-attacks like FDI or man-in-the-middle (MITM) that can modify measurements in a way evading traditional detection algorithms [106]. Mitigating these threats involves multi-layered cybersecurity measures incorporating encrypted data transfers, network segmentation, anomaly detection, and secure time synchronization protocols a non-trivial undertaking for control centers with legacy infrastructure constraints.

- Regulatory and Policy Framework Constraints

The incorporation of real-time inertia estimation into control operations could be in conflict with current regulatory and operational procedures. Control centers work under strict regulations, and the inclusion of automated inertia-calculation equipment could require changes to dispatch procedures, training for operators, and potentially the market rules that govern grid reliability. Although associations of the industry (e.g., ISGAN) welcome the prospect that synchrophasor applications may change, there remains a “confidence gap” between offline analytical use and application in mission-critical control operations [102]. This gap must be filled with coordination among vendors, system operators, and regulators to harmonize reliability norms, data sharing policy, and operational preparedness in anticipation of inertia-based decision-support tools.

- Computational Scalability and Hardware Constraints

To maintain such ML-based inertia estimators, particularly deep learning models or reinforcement-learning agents, in real time necessitates aggressive computations. The majority of control centers are constructed atop legacy hardware that isn’t intended to handle low-latency inference. There is some evidence from comparable real-time estimation tasks (for example, state estimation with deep unrolled neural networks) that running such models in real time can flood standard control-center hardware with no hardware acceleration [107]. Hence, achieving working deployment may be at the expense of such upgrades as edge processors, GPU-enabled servers, or compression of models for specific models—increasing cost and complexity in infrastructure. With no upgrades, computational overhead would nullify ML-based estimation’s responsiveness advantage and result in lagging or stale inertia estimates with diminished effectiveness for control decisions. This tradeoff calls for co-design of both ML models and deployment platforms that will deliver accuracy and efficiency.

- Adaptability of Evolving Grid Conditions

Power grids are increasingly variable with the increased presence of inverter-based sources, fluctuating load patterns, and dynamically changing network conditions. Historical or simulated data-trained ML models may deteriorate with changing system dynamics. ML-based inertia estimation literature identifies the importance of adaptability and resilience under changing inertia conditions [108]. In the absence of online or incremental learning ability, the estimators can drift, compromising accuracy and operator trust in the long run. For the sake of validity, estimation pipelines would be combined with adaptive methods such as continuous learning, drift detection, or sporadic retraining and validation pipelines. These enhancements do bring additional data management, validation, and governance complexity that needs to be managed for use in practice.

- Incomplete System Observability and PMU Placement

Successful inertia estimation demands proper system observability, which is contingent upon optimal placement of PMUs. Empirical Gramian-based observability methods have proven that optimal placement of PMUs significantly improves the robustness and accuracy of dynamic state estimation under normal operation conditions, even under contingencies and load changes [109]. Dispersing widely the deployment of PMUs is economically and logistically constraining for most utilities, and sparse or unbalanced coverage consequently results. Inadequate PMU placement is capable of causing blind zones or degraded estimator performance during important events. Addressing this challenge requires coordinated planning that integrates optimal placement, cost-effective deployment, and PMU expansion aligned with

Table 8
Summary of inertia estimation measurement-based methods.

Ref	Methods	System	Inertia contribution	Required system condition	Online/ Offline	Dependence/Error
[2]	Kalman filter	Italian Transmission Network	SGs	Ambient	Online	Error <8 % (avg. 2.5 %)
[14]	Swing eq. + ESPRIT	39 bus New England system	SGs	Disturbance	Online	Error 1.4–4.2 %
[26]	IEEE 39-bus & Gujarat grid	IEEE 39-bus & Gujarat grid	SGs, frequency and voltage-dependent load, VI	Disturbance	Offline/ Online	Error 4–7 %
[48]	Swing eq.	Great Britain power system	SGs + small/micro gen	Disturbance	Offline	Number of monitoring nodes and fault location: Error 0.5–7 %
[49]	Energy-based	Irish grid	SGs, power station auxiliary loads, WTs, load demand	Disturbance	Offline	Droop value: Error 0.7–2.5 %
[53]	Swing eq. + Least-Squares Method	Two-area system, The PST 16 benchmark test system	SGs	Disturbance	Online	Number of PMUs, type of perturbation, and load behavior: Error 0.5–13 %
[54]	*RoCoF* and ΔP_e estimations by Osplines method and *H* calculation by swing eq.	IEEE 9-bus and 68-bus systems, NETS-NYPS	SGs	Disturbance	Online	Load or generation disturbance: Error 0.01–1.5 %
[110]	Non-recursive system identification method	IEEE 39-bus network and the aggregated New Zealand network	SGs and VI from PMSG WTs	Ambient	Online	Error 2.4–3.8 % (the aggregated network), 8.5 % (real data)
[80]	Multivariate Random Forest Regression (MRFR)	Synchrophasor measurements of the U.S. WECC system from GridEye	SGs + VI from IBRs	Ambient	Online	Load changes: Error mean 3.1 %, max 8.7 %
[111]	Swing eq.	the SP Energy Networks, the Nordic power system	SGs	Disturbance	Offline	Load voltage-power dependence: Error 1–13 %
[9]	LRCN and GCN	IEEE 24-bus system	SGs + IBRs	Ambient (through Low level Probing Signal)	Online	Features extracted and number of PMUs: LRCN (2.66 %), GCN (1.85 %)
[56]	Transient frequency analysis and swing equation deformation: *First Stage* (ESPRIT) and *Second Stage* (WNLS approach)	IEEE 39-bus system, Taiwan Power Systems	SGs	Disturbance	Online	Load condition and the event disturbed with sufficiently small measurement noises: Error <2.5 %
[57]	Combines the phase difference and power exchange between interconnected areas	The 60 Hz Japanese power system	Generation and demand side (e.g., SGs, synchronous motors, induction motors, generator control effects)	Ambient	Online	Geographical location and rated capacity of the generator with the attached PSS: Error 0.08–7 %
[55]	Swing eq. + sDMD algorithm	Non-DFIG device (using the PV system as an example) and DFIG, which are both connected into a WPTCS parallel 4- Machine-2-Area system	Constant and time-varying inertia in non-synchronous devices (DFIG, PMSG, PV)	Disturbance	Online	Noise: Error 1–4 %.
[58]	Local rational model (LRM)	IEEE 39-bus system with CBRs, laboratory test	SGs, CBRs	Ambient	Online	Error 0.7–3.7 %
[60]	Covariance matrix	IEEE 39-bus system, 1479-bus model of the all-island Irish grid	SGs and VI from CIG	Ambient	Online	Error 0.14–5.4 %
[63]	System identification method	IEEE 39-bus system	SGs	Ambient	Online	Error 1–40 %
[65]	System-identification method	Microgrid network hosting a mix of RESs and BESS	VI in a microgrid system	Disturbance	Offline	Error 0.3–29 %
[66]	Iterative equation error system identification	IEEE 39-bus and the IEEE 118-bus test systems	SGs, CIG	Ambient and ringdown signal measurements (power imbalance events)	Online	Normal operation condition error 2–4.5 %, power imbalance event error 1.5–3.5 %
[76]	ARMAX model	IEEE 68-Bus power system, Real measurements from the NYPS	SGs	Disturbance	Offline	Disturbance location and size: Error 1–4.2 %

ESPRIT: estimation of signal parameter via rotational invariance techniques.
WT s: Wind turbines.
NETS-NYPS: New England transmission system and New York power system.
PMSG: permanent magnet SG.
SP: Scottish power.
WNLS: weighted nonlinear least square.
DFIG: doubly fed induction generator.
WPTCS: wind–photovoltaic–thermal coupling system.
CBRs: converter-based resources.

inertia estimation requirements, ensuring estimator reliability without excessive investment. Table 7 provides a summary of the challenges and remarks related to the implementation of continuous inertia estimation.

6. Summary

In this section, Table 8 summarizes the methods reported in the literature, comparing their accuracy and their consideration of inertia contributions from different sources. While it is difficult to identify a single method as the most accurate, given the variations in data sets and network configurations, certain characteristics of an accurate method can be outlined. With increasing CIG penetration, an accurate method should be capable of continuously estimating inertia contributions from SGs, CIGs, and the load side, under both normal operating conditions and during system disturbances. It should demonstrate a consistently low relative error (RE) across a wide range of operating scenarios and fault conditions, while maintaining stability in the presence of measurement noise and data uncertainty. Moreover, scalability to large, complex systems and adaptability to varying measurement infrastructures, such as diverse PMU placements, are critical for practical deployment.

7. Challenges and future perspective for renewable power system inertia estimation

Future initiatives should focus on creating user-friendly tools for measuring and forecasting inertia, while establishing standardized time windows for RoCoF assessments. Regular updates to frequency protection schemes are vital to adapt to changing grid dynamics. A balanced spatial distribution of inertia across regional grids/frequency control areas is essential, given that RoCoF values differ based on location and nearby inertia levels. Exploring the minimum synchronous inertia requirements, especially for systems with high-RES penetration and IBRs, is essential to ensure operational security. System studies should examine the impact of increased HVDC connections and critical scenarios, such as the sudden shutdown of multiple nuclear power plants, on system kinetic energy. Future inertia ancillary service market designs should carefully address regional allocation, co-optimization with frequency control services, and demand-side inertia integration, including the future expansion of electrical vehicle-to-grid schemes. Additionally, advanced modeling approaches should explore the combined optimization of energy and reserves to identify cost-effective resource allocation while considering non-convexities in production systems.

8. Conclusion

A comprehensive review of inertia estimation methods was conducted, categorizing them into model-based, measurement-based, and forecasting approaches. The study explored both academic insights and practical applications, including the use of artificial intelligence for online inertia estimation. Various methods were assessed through tables highlighting classification, advantages/disadvantages, and formulations. According to the literature, an effective inertia estimation method should be capable of continuously assessing inertia contributions from SGs, CIGs, and the demand side under both normal operating conditions and system disturbances. It should maintain a consistently low relative error across a wide range of scenarios, including varying operating points, load levels, and fault types and locations, thereby ensuring robustness and reliability for real-time monitoring and control applications. Furthermore, the method should be cost-effective, requiring minimal additional investment and avoiding the need for specialized equipment, while still enabling accurate online inertia estimation using the existing measurement infrastructure. In this regard, the iterative equation error system identification method has demonstrated the capability to operate with both ambient data and ringdown signal measurements, achieving high accuracy. Moreover, it can perform real-time inertia estimation for both SGs and CIGs, making it a practical candidate for deployment in modern power systems. However, it requires further analysis to assess its capability to estimate the load-side inertia contribution. Regarding machine learning–based methods reported in the literature, the dual-stage hybrid deep learning method combined with hybrid networks has demonstrated the capability to accurately estimate time-varying inertia under both ambient conditions and various disturbance scenarios. While its performance under simulated environments shows promising accuracy, further validation using real PMU measurements is necessary. Additionally, its current formulation does not explicitly account for the inertia contribution from CIGs, which should be incorporated to enhance its applicability in modern low-inertia power systems.

The ambient approach was emphasized for its ability to estimate inertia continuously under normal conditions and account for virtual inertia from converter-interfaced generators. However, challenges remained, particularly with data-driven methods that were sensitive to sampling data and difficulties in extracting inertia in model-based approaches. Future research should focus on factors like oscillatory components during transients, PMU types, and their location relative to the COI motion. Inertia estimation methods used by power companies aim to enhance the visibility of real-time system dynamics, especially in systems with high-RES penetration. Techniques such as probing signal-based estimation, real-time modulation, and frequency response analysis provide valuable insights, though challenges persist in ensuring accuracy and scalability in large grids or rapidly changing conditions. This study emphasizes the necessity of incorporating power system inertia requirements into security planning, particularly in grids with significant RES integration.

Declaration of competing interest

The authors declare that they have no known competing financial interests or personal relationships that could have appeared to influence the work reported in this paper.

Acknowledgments

This work was supported in part by the National Science and Technology Council of Taiwan under Grants NSTC 111-2923-E-992-001-MY3, NSTC 113-2218-E-992-003, and NSTC 114-2221-E-992-045.

Data availability

No data was used for the research described in the article.

References

[1] Jacobson MZ, et al. 100% clean and renewable wind, water, and sunlight all-sector energy roadmaps for 139 countries of the world. Joule 2017;1(1):108–21.
[2] Allella F, Chiodo E, Giannuzzi GM, Lauria D, Mottola F. On-line estimation assessment of power systems inertia with high penetration of renewable generation. IEEE Access 2020;8:62689–97.
[3] Nouti D, Ponci F, Monti A. Heterogeneous inertia estimation for power systems with high penetration of converter-interfaced generation. Energies 2021;14(16):5047.
[4] Zhang W, Wen Y, Li L, Zhang Q, Cheng C, Li J. Online estimation of inertia and frequency regulation capability based on small perturbation. Energy Rep 2022;8:650–6.
[5] Zhou T, Huang J, Quan H, Xu Y, Liu Z. Inertial security region estimation and analysis of new power systems considering renewable energy virtual inertial. Energy Rep 2023;9:1836–49.
[6] Carlini E, Del Pizzo F, Giannuzzi G, Lauria D, Mottola F, Pisani C. Online analysis and prediction of the inertia in power systems with renewable power generation based on a minimum variance harmonic finite impulse response filter. Int J Electr Power Energy Syst 2021;131:107042.
[7] Cui H, et al. Disturbance propagation in power grids with high converter penetration. Proc IEEE 2022;111(7):873–90.
[8] Tielens P, Van Hertem D. The relevance of inertia in power systems. Renew Sustain Energy Rev 2016;55:999–1009.

[9] Tuo M, Li X. Machine learning assisted inertia estimation using ambient measurements. IEEE Trans Ind Appl 2023;59(4):4893–903.
[10] Inoue T, Taniguchi H, Ikeguchi Y, Yoshida K. Estimation of power system inertia constant and capacity of spinning-reserve support generators using measured frequency transients. IEEE Trans Power Syst 1997;12(1):136–43.
[11] Chassin DP, Huang Z, Donnelly MK, Hassler C, Ramirez E, Ray C. Estimation of WECC system inertia using observed frequency transients. IEEE Trans Power Syst 2005;20(2):1190–2.
[12] Wall P, Gonzalez-Longatt F, Terzija V. Estimation of generator inertia available during a disturbance. In: 2012 IEEE power and energy society general meeting; 2012. p. 1–8. IEEE.
[13] Sun M, Feng Y, Wall P, Azizi S, Yu J, Terzija V. On-line power system inertia calculation using wide area measurements. Int J Electr Power Energy Syst 2019;109:325–31.
[14] Panda RK, Mohapatra A, Srivastava SC. Online estimation of system inertia in a power network utilizing synchrophasor measurements. IEEE Trans Power Syst 2019;35(4):3122–32.
[15] 3. ENTSO-E. Future system inertia. Available online:https://eepublicdownloads.entsoe.eu/clean-documents/Publications/SOC/Nordic/Nordic_report_Future_System_Inertia.pdf, ; 2018.
[16] ERCOT, Inertia: Basic concepts and impacts on the ERCOT grid, Technical Report, Apr. 2018. [Online]. Available: https://www.ercot.com/files/docs/2018 /04/04/ Inertia Basic Concepts Impacts On ERCOT v0.pdf.
[17] Heylen E, Teng F, Strbac G. Challenges and opportunities of inertia estimation and forecasting in low-inertia power systems. Renew Sustain Energy Rev 2021;147:111176.
[18] Dimoulias SC, Kontis EO, Papagiannis GK. Inertia estimation of synchronous devices: review of available techniques and comparative assessment of conventional measurement-based approaches. Energies 2022;15(20):7767.
[19] Ayamolowo OJ, Manditereza P, Kusakana K. An overview of inertia requirement in modern renewable energy sourced grid: challenges and way forward. J Electr Syst Inform Technol 2022;9(1):11.
[20] Tan B, Zhao J, Netto M, Krishnan V, Terzija V, Zhang Y. Power system inertia estimation: review of methods and the impacts of converter-interfaced generations. Int J Electr Power Energy Syst 2022;134:107362.
[21] Rezkalla M, Pertl M, Marinelli M. Electric power system inertia: requirements, challenges and solutions. Electr Eng 2018;100:2677–93.
[22] ENTSOE. Fast frequency reserve – solution to the nordic inertia challenge [Online]. Available: https://www.fingrid.fi/en/news/news/2019/report-fast-frequency-reserve–solution-to-the-nordic-inertia-challenge/; 2019.
[23] Fernández-Guillamón A, Vigueras-Rodríguez A, Molina-García Á. Analysis of power system inertia estimation in high wind power plant integration scenarios. IET Renew Power Gener 2019;13(15):2807–16.
[24] Wang F, Sun L, Wen Z, Zhuo F. Overview of inertia enhancement methods in DC system. Energies 2022;15(18):6704.
[25] Lavanya L, Swarup KS. Continuous real-time estimation of power system inertia using energy variations and Q-learning. IEEE Open J Instrument Measure 2023;2:1–11.
[26] Dhara PK, Rather ZH. Non-synchronous inertia estimation in a renewable energy integrated power system with reduced number of monitoring nodes. IEEE Trans Sustain Energy 2022;14(2):864–75.
[27] Cari EP, Landgraf TG, Alberto LF. A constrained minimization approach for the estimation of parameters of transient generator models. Elec Power Syst Res 2017;143:252–61.
[28] Tan B, Zhao J, Terzija V, Zhang Y. Decentralized data-driven estimation of generator rotor speed and inertia constant based on adaptive unscented Kalman filter. Int J Electr Power Energy Syst 2022;137:107853.
[29] Liu M, Chen J, Milano F. On-line inertia estimation for synchronous and non-synchronous devices. IEEE Trans Power Syst 2020;36(3):2693–701.
[30] Milano F, Ortega A. A method for evaluating frequency regulation in an electrical grid–Part I: theory. IEEE Trans Power Syst 2020;36(1):183–93.
[31] Vahidnia A, Ledwich G, Palmer E, Ghosh A. Generator coherency and area detection in large power systems. IET Gener Transm Distrib 2012;6(9):874–83.
[32] Wang B, Yang D, Cai G, Ma J, Chen Z, Wang L. Online inertia estimation using electromechanical oscillation modal extracted from synchronized ambient data. J Modern Power Syst Clean Energy 2020;10(1):241–4.
[33] Mehrzad A, Darmiani M, Mousavi Y, Shafie-Khah M, Aghamohammadi M. An efficient rapid method for generators coherency identification in large power systems. IEEE Open Access J Power Energy 2022;9:151–60.
[34] Jiangkai Peng JT, Koralewicz Przemyslaw, Mendiola Emanuel, Dong Shuan, Anderson Hoke. Kelsey horowitz. https://www.nrel.gov/docs/fy24osti/87925.pdf.
[35] https://www.fingrid.fi/globalassets/dokumentit/fi/sahkomarkkinat/reservit/fast-frequency-reserve-solution-to-the-nordic-inertia-challenge.pdf (accessed).
[36] Zografos D, Ghandhari M. Estimation of power system inertia. In: 2016 IEEE power and energy society general meeting (PESGM). IEEE; 2016. p. 1–5.
[37] Zografos D, Ghandhari M. Power system inertia estimation by approaching load power change after a disturbance. In: 2017 IEEE power & energy society general meeting; 2017. p. 1–5. IEEE.
[38] Zografos D, Ghandhari M, Eriksson R. Power system inertia estimation: utilization of frequency and voltage response after a disturbance. Elec Power Syst Res 2018;161:52–60.
[39] Zhu L, Farantatos E, Ramasubramanian D, Mitra P, Singhvi V, Elnasry M. Ambient PMU measurements based online regional inertia estimation and monitoring. In: 2024 international conference on smart grid synchronized measurements and analytics (SGSMA). IEEE; 2024. p. 1–5.
[40] Power System Operation Corporation (POSOCO). Indian Institute of Technology Bombay (IITB); 2022. https://posoco.in/wp-content/uploads/2022/01/Assessment-of-Inertia-in-Indian-Power-System.pdf.
[41] Brown M, Biswal M, Brahma S, Ranade SJ, Cao H. Characterizing and quantifying noise in PMU data. In: 2016 IEEE power and energy society general meeting (PESGM). IEEE; 2016. p. 1–5.
[42] Li D, Dong N, Yao Y, Xu B, Gao DW. Area inertia estimation of power system containing wind power considering dispersion of frequency response based on measured area frequency. IET Gener Transm Distrib 2022;16(22):4640–51.
[43] Cao X, Stephen B, Abdulhadi IF, Booth CD, Burt GM. Switching Markov Gaussian models for dynamic power system inertia estimation. IEEE Trans Power Syst 2015;31(5):3394–403.
[44] Zeng F, Zhang J, Chen G, Wu Z, Huang S, Liang Y. Online estimation of power system inertia constant under normal operating conditions. IEEE Access 2020;8:101426–36.
[45] Wang W, Yao W, Chen C, Deng X, Liu Y. Fast and accurate frequency response estimation for large power system disturbances using second derivative of frequency data. IEEE Trans Power Syst 2020;35(3):2483–6.
[46] Hu P, Li Y, Yu Y, Blaabjerg F. Inertia estimation of renewable-energy-dominated power system. Renew Sustain Energy Rev 2023;183:113481.
[47] Kuivaniemi M, et al. Estimation of system inertia in the Nordic power system using measured frequency disturbances. In: Cigre conference; 2015. p. 27–8.
[48] Ashton PM, Saunders CS, Taylor GA, Carter AM, Bradley ME. Inertia estimation of the GB power system using synchrophasor measurements. IEEE Trans Power Syst 2014;30(2):701–9.
[49] Best RJ, Brogan PV, Morrow DJ. Power system inertia estimation using HVDC power perturbations. IEEE Trans Power Syst 2020;36(3):1890–9.
[50] Tamrakar U, Shrestha D, Maharjan M, Bhattarai BP, Hansen TM, Tonkoski R. Virtual inertia: current trends and future directions. Appl Sci 2017;7(7):654.
[51] Bastiani BA, Oliveira RVd. Frequency dynamics of power systems with inertial response support from wind generation. Energies 2023;16(14):5280.
[52] Wang Y, Yokoyama A, Baba J. Online inertia estimation of power systems based on transient phasor data with weighted least squares method. In: 2023 IEEE belgrade PowerTech. IEEE; 2023. p. 1–6.
[53] Rossetto Moraes G, Ilea V, Berizzi A, Pisani C, Giannuzzi G, Zaottini R. A perturbation-based methodology to estimate the equivalent inertia of an area monitored by pmus. Energies 2021;14(24):8477.
[54] Rodales D, et al. Model-free inertia estimation in bulk power grids through O-splines. Int J Electr Power Energy Syst 2023;153:109323.
[55] Li Y, et al. Real-time estimation of time-varying inertia for non-synchronous devices using streaming dynamic mode decomposition. Int J Electr Power Energy Syst 2024;157:109847.
[56] Lee S-H, Liu J-H, Chen B-Y, Chu C-C. A two-stage data-driven method for estimating the system inertia utilizing event-driven PMU measurements. IEEE Trans Ind Appl 2023;59(5):5243–56.
[57] Kerdphol T, Watanabe M, Nishikawa R, Hayashi Y, Mitani Y. Inertia estimation of the 60 Hz Japanese power system from synchrophasor measurements. IEEE Trans Power Syst 2022;38(1):753–66.
[58] Mazidi M, McKelvey T, Chen P. A pure data-driven method for online inertia estimation in power systems using local rational model approach. IEEE Trans Ind Appl 2023;59(5):5506–16.
[59] Mehrzad A, et al. Ambient synchrophasor data-based power system inertia estimation using system identification method. In: 2025 IEEE industry applications society annual meeting (IAS); 2025. p. 1–5. IEEE.
[60] Bizzarri F, Del Giudice D, Grillo S, Linaro D, Brambilla A, Milano F. Inertia estimation through covariance matrix. IEEE Trans Power Syst 2023;39(1):947–56.
[61] Tuttelberg K, Kilter J, Wilson D, Uhlen K. Estimation of power system inertia from ambient wide area measurements. IEEE Trans Power Syst 2018;33(6):7249–57.
[62] Yang D, et al. Ambient-data-driven modal-identification-based approach to estimate the inertia of an interconnected power system. IEEE Access 2020;8:118799–807.
[63] Zeng F, Zhang J, Zhou Y, Qu S. Online identification of inertia distribution in normal operating power system. IEEE Trans Power Syst 2020;35(4):3301–4.
[64] Zhang J, Xu H. Online identification of power system equivalent inertia constant. IEEE Trans Ind Electron 2017;64(10):8098–107.
[65] Phurailatpam C, Rather ZH, Bahrani B, Doolla S. Estimation of non-synchronous inertia in AC microgrids. IEEE Trans Sustain Energy 2021;12(4):1903–14.
[66] Gotti D, et al. Inertia estimation of a power system area based on iterative equation error system identification. IEEE Trans Power Syst 2024;39(5):6469–81.
[67] Cui Y, You S, Liu Y. Ambient synchrophasor measurement based system inertia estimation. In: 2020 IEEE power & energy society general meeting (PESGM); 2020. p. 1–5. IEEE.
[68] Zicheng L, Zhou T, Chen Z, Wang Y, Wang Y. Minimum inertia demand estimation of new power system considering diverse inertial resources based on deep neural network. IET Energy Syst Integrat 2023;5(1):80–94.
[69] Linaro D, et al. Continuous estimation of power system inertia using convolutional neural networks. Nat Commun 2023;14(1):4440.
[70] Li H, et al. Ambient-frequency-data based system-level inertia estimation using physical equation and its practice on Hawaii islands. IEEE Trans Power Syst 2024;39(6):6948–59.
[71] Ashton P, Taylor G, Carter A, Bradley M, Hung W. Application of phasor measurement units to estimate power system inertial frequency response. In: 2013 IEEE power & energy society general meeting; 2013. p. 1–5. IEEE.

[72] Kerdphol T, Watanabe M, Nishikawa R, Tamaki T, Mitani Y. Determining inertia of 60 Hz Japan power system using PMUs from power loss event. In: 2021 IEEE Texas power and energy conference (TPEC). IEEE; 2021. p. 1–5.
[73] del Giudice D, Grillo S. Analysis of the sensitivity of extended kalman filter-based inertia estimation method to the assumed time of disturbance. Energies 2019;12 (3):483.
[74] Wall P, Terzija V. Simultaneous estimation of the time of disturbance and inertia in power systems. IEEE Trans Power Deliv 2014;29(4):2018–31.
[75] Kontis EO, Pasiopoulou ID, Kirykos DA, Papadopoulos TA, Papagiannis GK. Estimation of power system inertia: a Comparative assessment of measurement-Based techniques. Elec Power Syst Res 2021;196:107250.
[76] Lugnani L, Dotta D, Lackner C, Chow J. ARMAX-based method for inertial constant estimation of generation units using synchrophasors. Elec Power Syst Res 2020;180:106097.
[77] Albeladi F, Basulaiman K, Barati M. Enhancing system inertia estimation: multi-head Graph attention networks leveraging PMU measurements. In: 2024 IEEE Texas power and energy conference (TPEC); 2024. p. 1–6. IEEE.
[78] Ramirez-Gonzalez M, Sevilla FS, Korba P. Power system inertia estimation using A residual neural network based approach. In: 2022 4th global power, energy and communication conference (GPECOM). IEEE; 2022. p. 355–60.
[79] Muhammed AO, Isbeih YJ, El Moursi MS, Elbassioni K. Artificial intelligence (ai) advanced techniques for real-time inertia estimation in renewable-based power systems. IEEE Trans Ind Appl 2024;61(2):2604–19.
[80] Su Y, et al. An adaptive PV frequency control strategy based on real-time inertia estimation. IEEE Trans Smart Grid 2020;12(3):2355–64.
[81] ENTSO-E. Future system inertia 2. 2025. https://www.statnett.no/globalassets /for-aktorer-i-kraftsystemet/utvikling-av-kraftsystemet/nordisk-frekvensstabi litet/future-system-inertia-phase-2.pdf. [Accessed 16 August 2021].
[82] Paidi ER, Marzooghi H, Yu J, Terzija V. Development and validation of artificial neural network-based tools for forecasting of power system inertia with wind farms penetration. IEEE Syst J 2020;14(4):4978–89.
[83] Gonzalez-Longatt F, Acosta MN, Chamorro HR, Topic D. Short-term kinetic energy forecast using a structural time series model: study case of nordic power system. In: 2020 international conference on smart systems and technologies (SST). IEEE; 2020. p. 173–8.
[84] Heylen E, Browell J, Teng F. Probabilistic day-ahead inertia forecasting. IEEE Trans Power Syst 2021;37(5):3738–46.
[85] Ela E, Milligan M, Bloom A, Botterud A, Townsend A, Levin T. Evolution of wholesale electricity market design with increasing levels of renewable generation. 2014.
[86] Bian Y, Wyman-Pain H, Li F, Bhakar R, Mishra S, Padhy NP. Demand side contributions for system inertia in the GB power system. IEEE Trans Power Syst 2017;33(4):3521–30.
[87] Thiesen H, Jauch C. Determining the load inertia contribution from different power consumer groups. Energies 2020;13:1588.
[88] Chen T, Guo J, Chaudhuri B, Hui S. Virtual inertia from smart loads. IEEE Trans Smart Grid 2020;11(5):4311–20.
[89] Elenkova M, Asprou M, Hadjidemetriou L, Panayiotou CG. Estimation of load inertia using ambient measurements from synchrophasor technology. In: 2022 IEEE PES innovative smart grid technologies conference Europe. ISGT-Europe); 2022. p. 1–5.
[90] Li P, Hu W, Xu X, Huang Q, Liu Z, Chen Z. A frequency control strategy of electric vehicles in microgrid using virtual synchronous generator control. Energy 2019; 189:116389.
[91] Kazemtarghi A, Dey S, Mallik A. Optimal utilization of bidirectional EVs for grid frequency support in power systems. IEEE Trans Power Deliv 2022;38(2): 998–1010.
[92] Pandit D, et al. Frequency support from electric vehicles for advancing renewable energy integration. IEEE Trans Power Syst 2024;40(1):636–49.
[93] Abubakr H, Mohamed TH, Hussein MM, Guerrero JM, Agundis-Tinajero G. Adaptive frequency regulation strategy in multi-area microgrids including renewable energy and electric vehicles supported by virtual inertia. Int J Electr Power Energy Syst 2021;129:106814.
[94] Wu X, Huang H, Chen J, Tong X, Tong N, Lai LL. Consensus algorithm based two-stage frequency regulation strategy with EVs participating as VSMs. IEEE Trans Smart Grid 2025;16(2):1562–74.
[95] Ke S, et al. Consistency collaboration control strategy based on adaptive virtual inertia in multiple charging stations. IEEE Trans Energy Convers 2023;39(2): 896–913.
[96] Kerdphol T. Leveraging vehicle-to-grid technology for sharing synthetic inertia in renewable-dominant grids. Elec Power Syst Res 2025;241:111405.
[97] 1, Australian energy market operator (AEMO) [Online]. Available: https://arena. gov.au/knowledge-bank/reactive-technologies-system-inertia-measurement-de monstration/.
[98] 899. Australian Renewable Energy Agency (ARENA). https://arena.gov.au/pro jects/reactive-technologies-system-inertia-measurement-demonstration /(accessed).
[99] 7868. Oak Ridge National Laboratory (ORNL). https://www.ornl.gov/project /real-time-grid-inertia-monitoring (accessed).
[100] EPRI. https://www.epri.com/research/programs/067417/results/3002027272 (accessed).
[101] Essential reliability services: whitepaper on sufficiency guidelines. North American Electricity Reliability Corporation (NERC); 2016 [Online]. Available: https://www.nerc.com/comm/Oth er/pages/essential-reliability-services-task-force-(erstf).aspx.
[102] Uhlen K, Overholt P, Valentine O. Synchrophasor applications for wide area monitoring and control. ISGAN annex 2016;6.
[103] NERC. Reliability guideline, PMU placement and installation [Online]. Available: https://www.nerc.com/comm/RSTC_Reliability_Guidelines/Reliability%20Gui deline%20-%20PMU%20Placement.pdf; Dec. 2016.
[104] Blair SM, Syed MH, Roscoe AJ, Burt GM, Braun J-P. Measurement and analysis of PMU reporting latency for smart grid protection and control applications. IEEE Access 2019;7:48689–98.
[105] Shereen E. Security of time synchronization for PMU-based power system state estimation: Vulnerabilities and countermeasures. KTH Royal Institute of Technology; 2021.
[106] Abu-Rub OH, et al. Cybersecurity challenges in low-inertia power-electronics-dominated grids. IEEE Power Electr Magazine 2025;11(4):20–30.
[107] Zhang L, Wang G, Giannakis GB. Real-time power system state estimation and forecasting via deep unrolled neural networks. IEEE Trans Signal Process 2019;67 (15):4069–77.
[108] Heidari M, et al. A review on application of machine learning-based methods for power system inertia monitoring. Int J Electr Power Energy Syst 2024;162: 110279.
[109] Qi J, Sun K, Kang W. Optimal PMU placement for power system dynamic state estimation by using empirical observability Gramian. IEEE Trans Power Syst 2014;30(4):2041–54.
[110] Makolo P, Zamora R, Lie TT. Online inertia estimation for power systems with high penetration of RES using recursive parameters estimation. IET Renew Power Gener 2021;15(12):2571–85.
[111] Wilson D, Yu J, Al-Ashwal N, Heimisson B, Terzija V. Measuring effective area inertia to determine fast-acting frequency response requirements. Int J Electr Power Energy Syst 2019;113:1–8.